HHS Public Access

Author manuscript

J Neurol. Author manuscript; available in PMC 2017 October 01.

Published in final edited form as:

J Neurol. 2016 October ; 263(10): 1927–1938. doi:10.1007/s00415-016-8221-1.

ARTERIAL SPIN LABELING PERFUSION PREDICTS LONGITUDINAL DECLINE IN SEMANTIC VARIANT PRIMARY PROGRESSIVE APHASIA

Christopher A. Olm, MA[1], **Benjamin M. Kandel, BA**[2], **Brain B. Avants, PhD**[2], **John A. Detre, MD**[3], **James C. Gee, PhD**[2], **Murray Grossman, MD, EdD**[1], and **Corey T. McMillan, PhD**[1,*]

[1]Penn Frontotemporal Degeneration Center, Department of Neurology, University of Pennsylvania, Philadelphia, PA, USA

[2]Penn Image Computing and Science Lab, Department of Radiology, University of Pennsylvania, Philadelphia, PA, USA

[3]Departments of Neurology and Radiology, University of Pennsylvania, Philadelphia, PA, USA

Abstract

Objective—To evaluate the prognostic value of regional cerebral blood flow (CBF) measured by arterial spin labeled (ASL) perfusion MRI in patients with semantic variant primary progressive aphasia (svPPA).

Methods—We acquired pseudo-continuous ASL (pCASL) MRI and whole-brain T1-weighted structural MRI in svPPA patients (N=13) with cerebrospinal fluid biomarkers consistent with frontotemporal lobar degeneration pathology. Follow-up T1-weighted MRI was available in a subset of patients (N=8). We performed whole-brain comparisons of partial volume-corrected CBF and cortical thickness between svPPA and controls, and compared baseline and follow-up cortical thickness in regions of significant hypoperfusion and hyperperfusion.

Results—Patients with svPPA showed partial volume-corrected hypoperfusion relative to controls in left temporal lobe and insula. svPPA patients also had typical cortical thinning in anterior temporal, insula, and inferior frontal regions at baseline. Volume-corrected hypoperfusion was seen in areas of significant cortical thinning such as the left temporal lobe and insula. Additional regions of hypoperfusion corresponded to areas without cortical thinning. We also observed regions of hyperperfusion, some associated with cortical thinning and others without cortical thinning, including right superior temporal, inferior parietal, and orbitofrontal cortices. Regions of hypoperfusion and hyperperfusion near cortical thinning at baseline had significant longitudinal thinning between baseline and follow-up scans, but perfusion changes in distant areas did not show progressive thinning.

*Corresponding Author: Corey McMillan, University of Pennsylvania Perelman School of Medicine, Department of Neurology, 3 West Gates, Philadelphia, PA 19104, mcmillac@upenn.edu p. 215.764.0159.

Ethical Considerations: Prior to inclusion in the study, all participants participated in a written informed consent procedure under a protocol approved by the Institutional Review Board at the University of Pennsylvania in accordance with the ethical standards laid down in the 1964 Declaration of Helsinki and its later amendments.

Conflict of Interest: On behalf of all authors, the corresponding author states that there is no conflict of interest.

Conclusion—Our findings suggest ASL MRI may be sensitive to functional changes not readily apparent in structural MRI, and specific changes in perfusion may be prognostic markers of disease progression in a manner consistent with cell-to-cell spreading pathology.

Search Terms

Frontotemporal degeneration; semantic variant primary progressive aphasia; arterial spin labeling; MRI; functional neuroimaging

INTRODUCTION

Semantic variant primary progressive aphasia (svPPA) is a progressive neurodegenerative condition associated with frontotemporal degeneration (FTD). Clinically, svPPA is characterized by impaired naming, poor word comprehension, and degraded object knowledge with relatively preserved speech fluency [1, 2]. Neuroimaging studies, including structural magnetic resonance imaging (MRI) and functional FDG-PET modalities, suggest a characteristic distribution of disease in svPPA that is focused in left anterior and inferior temporal cortex [1, 3–7]. Cross-sectional studies show this area has widespread connectivity, including regions of modality-specific association cortex [8]. Longitudinal structural imaging studies of svPPA show progression of thinning posteriorly into the temporal lobe, dorsally into the inferior frontal lobe, and increasingly involving the contralateral anterior temporal lobe [9]. However, little is known about the prognostic value of functional changes in svPPA at baseline and how these relate to longitudinal structural changes. In this study, we examined the relationship between structural and functional imaging in cross-sectional and longitudinal MRI studies of svPPA.

Arterial spin labeling (ASL) is a functional MRI technique that quantitatively measures regional cerebral blood flow (CBF). ASL has been shown to coincide well with PET metabolism in patients with svPPA [10]. Moreover, ASL has advantages over PET methods for measuring brain function, including functional and structural imaging in the same scanning session, the lack of ionizing radiation associated with PET, and lower cost [11]. ASL has previously been used to investigate neurodegeneration in patients with MCI, AD, and FTD [12–15]. However, the relative utility of ASL MRI for predicting longitudinal cortical alterations has yet to be assessed. Past work has explored the importance of examining the differences, as well as the similarities, between functional and structural findings [15, 16]. Areas of functional hypoperfusion corresponding to thinning in cortical structures may reflect co-occurring functional and structural decline of a neuronal population. Areas of hypoperfusion also may be seen in regions without structural thinning. This may be an early indicator of a vulnerable brain region that will show cortical thinning in the future, or may occur due to diaschisis phenomena where there may be the appearance of reduced functioning in healthy areas that are receiving compromised projections from diseased areas [17]. Areas of hyperperfusion may also be seen in the setting of normal cortical volume or cortical thinning, and this too may reflect a compensatory increase in function in areas vulnerable to impending decline [13, 14]. Anatomically, functional changes in the setting of normal cortical thickness may occur in areas adjacent to regions of cortical thinning, consistent with a cell-to-cell pattern of spreading neuropathology [18, 19], or may

occur in distant regions [20, 21]. Longitudinal studies thus may reveal the prognostic value of functional imaging in svPPA.

We compared cortical thickness derived from T1-weighted MRI and volume-corrected CBF derived from a pseudo-continuous ASL (pCASL) technique [22]. We hypothesized that cross-sectional whole-brain comparisons between svPPA patients and healthy aging controls would reveal significant cortical thinning, hypoperfusion, and hyperperfusion. Thus, we expected to find regions of co-occurring cortical thinning and hypoperfusion, as well as co-occurring cortical thinning and hyperperfusion. Furthermore, we expected regions of hypoperfusion and hyperperfusion in areas with normal cortical thickness. We also investigated the dynamics of longitudinal decline in this progressive neurodegenerative condition by examining longitudinal gray matter (GM) structural changes in areas of hyperperfusion and hypoperfusion. We expected that specific areas of changed perfusion would be associated with longitudinal GM thinning and thus could serve as prognostic markers of neurodegeneration and help clarify the mechanism for disease progression.

METHODS

Participants

We evaluated 13 (7 female) svPPA patients from the Penn Frontotemporal Degeneration Center and Cognitive Neurology Clinic at the University of Pennsylvania and 19 (12 female) demographically-comparable healthy seniors. To be included in the study, patients were diagnosed with svPPA by a board-certified neurologist based upon published criteria [23], showed minimal to no vascular disease on a clinical T2 image, were native English speakers, and demonstrated a neuropsychological profile consistent with svPPA (table 1). Each patient had a cerebrospinal fluid (CSF)-derived total-tau-to-beta-amyloid-1–42 ratio of <0.34, and thus was considered in this context to have likely FTLD pathology [24]. Participants completed T1-weighted and resting pCASL MRI in the same scanning session with coverage including the temporal pole and the vertex. Prior to inclusion in the study, all participants participated in a written informed consent procedure under a protocol approved by the Institutional Review Board convened at the University of Pennsylvania in accordance with the ethical standards laid down in the 1964 Declaration of Helsinki and its later amendments.

A subset of the svPPA participants (N=8) also had a follow-up T1-weighted MRI, on average 13.25 months (range=10–20 months) after the initial scan. These patients were demographically and cognitively representative of the baseline svPPA cohort and had cortical thickness representative of the baseline cohort in the regions examined for the longitudinal analysis (supplementary table e-1; supplementary figure e-1). The remaining svPPA patients did not have a follow-up scan for a variety of reasons (e.g., intercurrent illness, death, unwillingness to participate due to disease progression, transportation difficulty). We attempted follow-up pCASL MRI for all patients, however, with limited availability of data due to poor data quality, we deemed a follow-up perfusion analysis with such a small group unreasonable.

MRI Acquisition and Processing

Images were collected using a 3T Siemens Tim Trio scanner with an 8-channel head coil. Sessions started with a high-resolution T1-weighted MPRAGE structural scan, with TR=1620ms, TE=3.09ms, flip angle=15°, 192×256 matrix, and 1×1×1mm voxels. We processed T1 MRI images using antsCorticalThickness, [25] using highly accurate [26] Advanced Normalization Tools (ANTs) [27, 28]. Briefly, we deformed each dataset into a standard local template space, registering images into this space using a diffeomorphic deformation that is symmetric to minimize bias toward the reference space, and topology-preserving to capture the large deformation necessary to aggregate images in a common space. The ANTs Atropos tool uses template-based priors to segment images into 6 tissue classes (cortex, white matter, CSF, subcortical gray structures, midbrain, and cerebellum) and generate probability maps of each tissue. Next, cortical thickness was calculated [29] and then the cortical gray matter probability (GMP), white matter probability (WMP), and cortical thickness images were transformed into $1mm^3$ resolution in MNI space and smoothed using a 5mm full-width half-maximum Gaussian kernel.

In the same scanning session as T1 acquisition, 80 volumes (40 tag, 40 control) of a spin echo echoplanar pCASL sequence were collected with TR=4300ms, TE=20ms, labeling duration=1500ms, post-label delay=1500ms, matrix=96×96, flip angle=90°, 2.5×2.5mm in-plane resolution, and 5mm thick slices with a 1mm slice gap, total: 20 slices. We removed the last 10 images in each series to minimize a previously reported frequency-dependent lipid artifact associated with a similar pCASL sequence [30]. The remaining pCASL images were processed using the antsASLProcessing script in ANTsR, as previously published [15]. Briefly, each pCASL volume was motion-corrected to the mean pCASL image. Next, we transformed each participant's T1 data into native pCASL space using affine registration. Using R (http://www.r-project.org/), a binary tag-control label, motion, and physiological confounds were regressed out of each volume [31]. We then quantified CBF using the formula:

$$f = \frac{\lambda * \Delta M}{2\alpha * M_0 * T_{1b} * \left(e^{-w/T_{1b}} - e^{-(\tau+w)/T_{1b}}\right)}$$

Where ΔM is the mean tag-control difference, λ is the blood/tissue water partition coefficient (0.9g/ml), α is the labeling efficiency for pCASL (85%), M_0 is the equilibrium magnetization estimated by averaging the control images, T_{1b} is the T1 relaxation time of blood (1664 ms), w is the post-labeling delay, and τ is the labeling duration (1500 ms). For analysis, we resampled each participant's mean CBF image to $1mm^3$ voxels to match the T1 resolution, transformed it into MNI space, and then smoothed it using a 5mm full-width half-maximum Gaussian kernel.

Partial volume effects are an important consideration when evaluating pCASL data given the relatively large acquired voxel size (2.5×2.5×5mm) that may include multiple tissues classes. To minimize potential confounds associated with these effects we used a previously reported correction method that accounts for the relative probabilities of a voxel being GM, WM, CSF, or some combination, and the expected relative contributions of the tissues to the raw

CBF signal [32]. As WM CBF is approximately 40% of GM CBF and CSF should account for 0% of CBF, we calculated partial volume corrected CBF (CBF_{PVC}) with the previously reported formula: CBF_{PVC}=CBF/(GMP+0.4*WMP) [32]. To account for registration imperfections due to differences in T1 and pCASL acquisition voxel size, we smoothed the (GMP+0.4*WMP) and CBF images before dividing when creating the CBF_{PVC} image, which was performed in MNI152 space. Finally, we calculated the mean CBF_{PVC} of the cortex and used this value to normalize each individual's CBF_{PVC} image to their own mean cortical perfusion level to create a corrected-CBF (CBF_{cor}) image.

Statistical Analysis

Demographic and neuropsychological statistics were computed using packages implemented in R (https://cran.r-project.org/). We used the *randomise* tool in FSL (http://fsl.fmrib.ox.ac.uk/fsl/randomise/) to perform nonparametric, permutation-based statistical analysis (permutations=10,000), which is equivalent to an error-corrected contrast, in order to compare svPPA patient and control cortical thickness, CBF, and CBF_{cor} images [33]. As there were no significant differences between age and gender distribution between patient and control groups, and we assume disease effects to be larger that those due to these factors, we did not remove these effects from our model. All comparisons were explicitly masked using the same mask generated by averaging all participant cortical thickness images and including voxels with a group mean thickness of greater than 0.4. For the cortical thickness comparison, we used a threshold of $p<0.0001$ (uncorrected) and considered clusters with a volume of greater than $500mm^3$. We use state-of-the-art data cleaning to process the images but the signal-to-noise ratio of ASL data is inherently low. This fact, matched with the different acquisition voxel sizes and many other factors, result in differences in statistical properties of the T1- and pCASL-derived datasets. Therefore, we used a less strict threshold for the CBF_{cor} comparisons than for the cortical thickness comparisons, considering clusters with a peak voxel $p<0.01$ (uncorrected) with a volume of greater than $500mm^3$ significant (no clusters reached significance when using the threshold $p<0.0001$ or when correcting for multiple comparisons).).

Longitudinal GM ROI Comparisons

Follow-up T1 MRIs were available for a subset of svPPA patients and were processed using the same procedure as above. We compared GM thickness between the two time-points in five ROIs, including the regions of significant baseline GM thinning, hypoperfusion partially overlapping baseline GM thinning, hypoperfusion distant from baseline GM thinning, hyperperfusion partially overlapping baseline GM thinning, and hyperperfusion distant from baseline thinning. Regions were considered "overlapping" if a cluster of volume-corrected hypo- or hyperperfusion had any voxels overlapping or within 1 cm (Euclidian distance) of a region of cortical thinning. All "distant" hypo- and hyperperfusion clusters were more than 2 cm from regions of cortical thinning (there were no clusters of hypo- or hyperperfusion between 1 and 2 cm from regions of cortical thinning). To account for variability in duration between baseline and follow-up scans among svPPA patients, the follow-up thickness values were transformed to represent annual change. The transformation consisted of calculating a monthly change, dividing the mean individual ROI thickness difference values by the number of months between the two scans, then multiplying this monthly by 12 to estimate

annual change. To determine whether or not there was a main effect of region on cortical thinning we performed a repeated measures ANOVA. After finding a significant main effect (reported below), we wanted to investigate which of the regions displayed cortical thinning. Thus, we performed paired-samples t-tests of cortical thickness between the two timepoints within each of the regions separately, and considered results significant at $p<0.05$. Comparisons were also made using the raw (i.e., not-annualized) changes.

Longitudinal Neuropsychological Analysis

Follow-up neuropsychological data (MMSE) was also available for the subset of svPPA patients who participated in the longitudinal imaging analysis (there was not a full data set for any other assessment). Similar to the longitudinal GM analysis, we performed analysis of annualized paired differences of the neuropsychological scores, considering results significant at $p<0.05$. We then investigated whether a significant correlation could be found between a change in MMSE and the cortical thickness differences, considering significant correlations with $p<0.05$.

RESULTS

Baseline Structural GM Comparisons

Patients with svPPA displayed significant cortical thinning relative to controls at baseline (figure 1; table 2), voxels with peak significance were located in temporopolar (BA 38; right t=9.36) and inferior temporal cortex (BA 20; left t=21.9, right t=6.00), with clusters extending to include bilateral middle temporal (BA 21) and superior temporal (BA 22) cortices. Clusters also extended to fully include the left temporopolar cortex, as well as into the left insula and orbitofrontal cortex (BA 11). Overall, there were more total suprathreshold voxels on the left compared to the right and the left cluster peak t value exceeded that of the clusters on the right. See Table 2 for a summary of results.

Baseline Perfusion Comparisons

Voxel-wise comparisons of raw perfusion were largely similar to the cortical thickness comparisons, as shown in Figure 2. We observed a clusters of reduced CBF with peak significance in the inferior portion of the left medial temporal cortex (BA 20; t=6.56) and left dorsolateral prefrontal cortex (BA 46; t=3.63) that extend to left anterior, middle, and superior temporal cortices, as well as supramarginal and insular cortx, in addition to anterior cingulate, orbitofrontal, middle, and inferior frontal cortices. Other peak differences located in the left hemisphere were in occipital lobe (BA 18; t=4.45) and medial frontal cortex (BA 8; t=3.45) and the right hemisphere in the anterior insula (t=3.40), orbitofrontal (BA 11; t=4.44), inferior medial temporal (BA 20; t=5.32), supramarginal (BA 39; t=5.11), anterior cingulate (BA 24; t=3.37), prefrontal (BA 10; t=3.53), medial motor (BA 4; t=3.56), and parahippocampal (BA 27; t=5.97) cortices, which extended to include bilateral posterior cingulate and precuneus, as well as right inferior and middle temporal cortices. No regions of hyperperfusion were found before correction for partial volume effects.

Voxel-wise comparisons of perfusion corrected for partial volume effects are displayed in Figure 1. We observed volume-corrected hypoperfusion with peak statistical values in left

middle temporal cortex (BA 21; t=5.41) as well as both anterior and posterior insula (t=3.77, t=3.98, respectively), with significant clusters extending to include left superior temporal cortex. Other peak voxels in the volume-corrected hypoperfusion analysis we in left precuneus (BA 7; t=3.80) and right posterior cingulate (BA 23; t=4.40), with clusters extending into right precuneus and left posterior cingulate.

We also observed regions of volume-corrected hyperperfusion in patients, with peak differences in right middle temporal cortex (BA 21; t=4.98) and right temporopolar cortex (BA 38; t=4.66) that extended into right orbitofrontal cortex. Another area of observed volume-corrected hyperperfusion was right inferior parietal cortex (BA 40; t=4.34). See Table 2 for a summary of results.

Baseline Structural GM and Corrected Perfusion Relationships

We observed 5 distinct patterns of structure and partial-volume-corrected function differences based upon our whole brain voxel-wise comparisons. One is regions that displayed thinning and no change in perfusion (shown in blue in Figure 1). The second is regions displaying volume-corrected hypoperfusion and co-occurring GM thinning, these regions included the left anterior and posterior insula, as well as middle and superior temporal cortices (Figure 1A). The third category is comprised of regions that displayed volume-corrected hypoperfusion that were distant from regions of cortical thinning and included bilateral precuneus and posterior cingulate cortex (Figure 1A). The fourth pattern consists of regions of volume-corrected hyperperfusion overlapping cortical thinning, such as the right orbitofrontal cortex and the right temporopolar and middle temporal cortices (Figure 1B). The fifth and final region is comprised of a cluster displaying hyperperfusion that is distant from any region of cortical thinning, located in right inferior parietal cortex (Figure 1B).

Longitudinal GM Comparisons

To evaluate whether the observed perfusion patterns predicted future cortical thinning, we examined annual cortical thickness change in the subset of svPPA patients with longitudinal data. We calculated annual mean cortical thickness change in five different regions that were determined using results from each of the whole-brain analyses, 1. GM thinning at baseline, 2. hypoperfusion partially overlapping baseline cortical thinning, 3. hypoperfusion distant from baseline areas of cortical thinning, 4. hyperperfusion partially overlapping baseline cortical thinning, and 5. hyperperfusion distant from baseline areas of cortical thinning. Using repeated measures ANOVA we found there was a significant main effect for region ($F(4)=3.581$; $p=0.018$). After finding that all differences passed Shapiro-Wilk normality tests (all $W>0.92$; $p>0.44$), we assumed our data was normal and thus used paired-samples t-tests to further explore which regions specifically displayed cortical thinning over time. As displayed in Figure 33, patients with svPPA displayed significant progressive thinning in regions of GM thinning at baseline ($t(7)=4.012$; $p=0.005$), in regions of partial volume-corrected hypoperfusion partially overlapping areas of baseline cortical thinning ($t(7)=2.834$; $p=0.025$), and in regions of partial volume-corrected hyperperfusion partially overlapping baseline areas of cortical thinning ($t(7)=2.542$; $p=0.039$). Regions of partial volume-corrected hypoperfusion distant from baseline areas of GM thinning and regions of partial

volume-corrected hyperperfusion distant from baseline areas of cortical thinning did not show significant progressive cortical thinning ($t(7)=0.003$; $p=0.998$ and $t(7)=1.249$; $p=0.251$, respectively). Results of raw (not annualized) paired-samples cortical thickness comparisons between baseline and follow-up showed a similar statistical pattern to that of the annualized results (see supplementary table e-2).

Longitudinal Neuropsychological Analyses

To evaluate changes in cognition over time, we performed paired tests of MMSE scores, finding a significant decrease between baseline and follow-up evaluation ($t(7)=2.509$; $p=0.040$). Change in MMSE was deemed to have a trending toward non-normal distribution by Shapiro-Wilk test ($W=0.846$; $p=0.0858$). We therefore used Spearman correlations to evaluate whether change in MMSE correlated with change in cortical thickness in any of the 5 regions and found no regions were significantly correlated ($rho<0.596$; $p>0.127$).

DISCUSSION

In the present study, we compared whole brain T1-weighted and partial volume-corrected ASL scans of svPPA patients and controls. Prior work suggests ASL MRI may be useful as a diagnostic marker in FTD, [10–14] and here we performed a detailed analysis of the relationship between structural and functional imaging in svPPA to examine its prognostic value. We observed five distinct imaging patterns of ASL function and GM structure, and evaluated these regions in longitudinal studies. We found that regions of partial volume-corrected hypoperfusion and hyperperfusion that partially overlap the core areas of baseline GM thinning exhibit significant longitudinal GM thinning, indicating that functional changes in some regions are preceding structural changes. Hypoperfusion and hyperperfusion also were seen in areas without co-occurring baseline GM thinning, distant from core areas of baseline cortical thinning. However, we did not observe longitudinal GM thinning in these areas, and these perfusion changes may reflect a process like diaschisis where there is only indirect CBF change due to projections from areas of significant disease. We also found that patients displayed a significant decrease in performance on neuropsychological measures between baseline and follow-up. These findings suggest that ASL changes in areas adjacent to baseline atrophy provide prognostic information predicting future regional cortical disease in svPPA, [10, 11, 13] and are consistent with a pattern of cell-to-cell prion-like spread in neurodegenerative disease [18, 19]. In the following sections we discuss each of these issues.

We observed a typical core anatomic distribution of GM thinning in svPPA [1, 3]. Substantial cortical thinning in svPPA is attributed to neuronal dropout associated with histopathologic burden in FTLD seen at autopsy. We found that the regions of cortical thinning at baseline yielded even further thinning at follow-up, similar to past structural MRI findings [9]. We used ASL to examine functional neural activity, as well. There was large correspondence of the uncorrected ASL data with the cortical thickness, and all regions of partial volume corrected hypoperfusion corresponded to regions of uncorrected hypoperfusion. Therefore, we felt it prudent to focus on the results of the partial volume corrected perfusion comparisons to minimize the risk of detecting reduced perfusion only

because of the reduced GM volume in the associated area. At baseline, most areas of observed GM thinning did not have corresponding changes in perfusion after partial volume correction, suggesting that the partial volume correction effectively normalized CBF for the amount of GM thinning. This implies that CBF and cortical thickness in these regions may be declining proportionately. It is unlikely that there is normal perfusion in these areas of GM thinning since hypoperfusion was extensive in these areas in uncorrected CBF maps (supplementary figure e-2), and these regions have previously been shown to have PET glucose hypometabolism in patients with svPPA [4, 5, 7]. Nonetheless, the partial volume correction approach used in this study to examine structure-function relationships in patients with svPPA relied on an assumed ratio between GM and WM CBF, and future studies should examine other methods of partial volume correction [15].

After partial volume correction, we observed hypoperfusion in areas overlapping and immediately adjacent to these core regions of GM thinning. Concurrent partial volume-corrected hypoperfusion and GM thinning may indicate that cortex has disproportionately reduced functioning relative to the amount of thinning. The left temporal region demonstrated hypoperfusion that extends posteriorly from the core area of GM thinning in the left temporal lobe. This area has been associated with poor performance on tasks designed to evaluate naming ability in patients with FTD [2] and following stroke [34]. Functional neuroimaging studies in healthy adults also implicate this area in, among other things, lexical semantic processing, a core clinical feature of svPPA [35]. Reduced functioning in this area may contribute to the impairments in these patients involving naming and word comprehension. The insula is another core area of cortical thinning where hypoperfusion extends in a superior direction. fMRI studies in healthy adults suggest that one role of the insula is contributing to social and executive functioning [36, 37] and other studies indicate that insula may be an area of early disease in FTD [18, 38]. Reduced function in the insula may contribute to behavioral changes that may be seen in svPPA [39]. We hypothesize that function in this area may have declined disproportionately and beyond that which can be detected only by examination of GM thickness. If true, these areas of hypoperfusion in regions of normal GM thickness may represent areas vulnerable to cell-to-cell spread of disease. Indeed, these areas demonstrated progressive GM thinning longitudinally, consistent with progressive neurodegeneration. Additional, pathology-based staging studies are needed to confirm this mechanism.

We also observed areas of corrected hypoperfusion that are distant from regions of core GM thinning, including posterior cingulate cortex, a region of hypometabolism found in past work using FDG-PET [4]. An account for hypoperfusion in the absence of GM thinning is diaschisis [17]. By this account, anatomic disease in one area may affect another functionally linked area without apparent structural thinning because interrupted white matter projections from an area of disease may result in reduced metabolic functioning in the otherwise intact projection zone. One such example may be hypoperfusion of precuneus, an area without GM thinning, due to damaged projections from the atrophied anterior temporal lobe via the inferio-lateral aspect of the cingulum. Hypoperfusion due to diaschisis in a structurally intact area is not expected to be associated with progressive thinning since the region of hypoperfusion is not diseased, and we did not see longitudinal thinning in these areas. We cannot rule out the possibility that hypoperfusion of a structurally intact region

may precede thinning on a time-scale longer than that examined in the present study. Future work should be performed to determine more precisely the mechanism underlying functional brain changes such as these with longer follow-up.

Hyperperfusion has been reported previously in FTD when using a similar normalization method [40], but the significance of this change was unclear. One possible explanation for hyperperfusion is that, early in the course of neurodegeneration, cortical regions may be able to increase activity to compensate for some neuronal death in the neuronal population. If true, such regions may show progressive thinning at follow-up. In fact, we observed several areas of hyperperfusion adjacent to and overlapping core regions of GM thinning that displayed progressive thinning longitudinally, namely, the right temporal lobe and orbitofrontal cortex. Past work has found cortical thinning in these areas over time in svPPA [6, 9]. Hyperperfusion in these regions thus may be consistent with compensatory increases in the functioning of mildly diseased brain regions early in the course of neurodegeneration. These right frontal and temporal regions have been associated with social rules and reward, among other functions [36, 37]. Partial volume-corrected hyperperfusion in these areas may explain in part why, at least in the early stages of disease, there is only modest evidence of personality and social changes in svPPA [41]. It is worth noting regions of corrected hyperperfusion showed a numerically larger mean change than the regions of corrected hypoperfusion, suggesting that regions of hyperperfusion may be at risk of more dramatic loss of cortex than those of hypoperfusion.

An alternative explanation for hyperperfusion, based on work using transcranial magnetic stimulation to study recovery of language processing following stroke, has suggested functional up-regulation in a contralateral homologue of a diseased region to provide compensatory support [42]. These are areas without underlying disease, and thus should not show longitudinal GM thinning. Patients with svPPA showed hyperperfusion in parietal cortex, distant from regions showing GM thinning, and this area did not show progressive thinning. Functions supported by this area correspond to several abilities that are relatively preserved in the course of svPPA, including visuospatial processing [1] and calculations [43]. The apparent absence of longitudinal GM thinning in this region is most consistent with functional up-regulation in the absence of neurodegenerative disease, and additional work is needed to determine the basis for hyperperfusion and whether this may also contribute to functional compensation.

We also found that MMSE decreased over time in these patients, indicating that the patients are indeed still showing progressive disease. We believe this is evidence there is value in identifying regions at risk for future cortical thinning. However, we were not able to identify a specific region associated with the changes in MMSE. Future studies should explore more specifically the changes in behavior over time and their structural and functional correlates in patients with svPPA.

There are some limitations to the current study. We studied well-characterized, pathologically-homogeneous patients with a rare condition, yet our sample size is somewhat small. Statistical results corrected for multiple comparisons are more robust than uncorrected results; however, our findings are in hypothesis-driven regions. Although longitudinal

studies of these rare patients are uncommon, our period of longitudinal follow-up was only about one year, and lengthier follow-up is needed to determine whether additional areas of GM thinning become evident. Partial volume effects represent a major confound in any functional imaging study. If the patient group has a global reduction of CBF, then mean-centering the signal may result in some areas with preserved CBF to display artifactually increased perfusion. Others have suggested that signal adjustment using the mean cortical measurement is an appropriate method for making differential diagnosis when using PDG-PET in neurodegenerative patients, although this may be confounded by other non-specific sources impacting ASL such age [40]. While we observed perfusion change in svPPA, additional work is needed to determine why some areas show hypoperfusion and others hyperperfusion.

With these caveats in mind, we conclude that partial volume-corrected hypoperfusion and hyperperfusion are present in svPPA patients. Some regions of changed perfusion overlap with structural GM thinning and others do not. Longitudinal imaging revealed progressive thinning only in areas of changed perfusion that are adjacent to regions with GM thinning at baseline. This is consistent with a model of longitudinal neurodegenerative progression that involves cell-to-cell disease spread. Moreover, as treatment trials emerge for FTD spectrum diseases, it is increasingly important to identify early markers of disease that can be monitored for therapeutic efficacy in the context of clinical trials, and to adjust parameters of imaging endpoints accordingly. ASL, together with structural imaging, may serve as an informative prognostic marker of disease progression.

Supplementary Material

Refer to Web version on PubMed Central for supplementary material.

Acknowledgments

This work was supported in part by the National Institutes of Health: AG017586, AG043503, AG015116, NS044266, AG032953, the Wyncote Foundation, and the Arking Family Foundation. Open-source ANTs software, available at https://github.com/stnava/ANTs, was used to process T1 and pCASL images. No funding source played a role in the study design, in the collection, analysis and interpretation of the data, in the writing of the report, or in the decision to submit the paper for publication.

REFERENCES

1. Hodges JR, Patterson K, Oxbury S, Funnell E. Semantic dementia: progressive fluent aphasia with temporal lobe atrophy. Brain. 1992; 115:1783–1806. [PubMed: 1486461]
2. Grossman M, McMillan C, Moore P, et al. What's in a name: voxel-based morphometric analyses of MRI and naming difficulty in Alzheimer's disease, frontotemporal dementia and corticobasal degeneration. Brain. 2004; 127:628–649. [PubMed: 14761903]
3. Whitwell JL, Avula R, Senjem ML, et al. Gray and white matter water diffusion in the syndromic variants of frontotemporal dementia. Neurology. 2010; 74:1279–1287. [PubMed: 20404309]
4. Drzezga A, Grimmer T, Henriksen G, et al. Imaging of amyloid plaques and cerebral glucose metabolism in semantic dementia and Alzheimer's disease. Neuroimage. 2008; 39:619–633. [PubMed: 17962045]
5. Diehl J, Grimmer T, Drzezga A, et al. Cerebral metabolic patterns at early stages of frontotemporal dementia and semantic dementia. A PET study. Neurobiol Aging. 2004; 25:1051–1056. [PubMed: 15212830]

6. Desgranges B, Matuszewski V, Piolino P, et al. Anatomical and functional alterations in semantic dementia: A voxel-based MRI and PET study. Neurobiol Aging. 2007; 28:1904–1913. [PubMed: 16979268]
7. Nestor PJ, Fryer TD, Hodges JR. Declarative memory impairments in Alzheimer's disease and semantic dementia. Neuroimage. 2006; 30:1010–1020. [PubMed: 16300967]
8. Guo CC, Gorno-Tempini ML, Gesierich B, et al. Anterior temporal lobe degeneration produces widespread network-driven dysfunction. Brain. 2013; 136:2979–2991. [PubMed: 24072486]
9. Rohrer JD, McNaught E, Foster J, et al. Tracking progression in frontotemporal lobar degeneration: Serial MRI in semantic dementia. Neurology. 2008; 71:1445–1451. [PubMed: 18955688]
10. Corouge I, Esquevin A, Lejeune F, et al. Arterial Spin Labeling at 3T in semantic dementia: perfusion abnormalities detection and comparison with FDG-PET. Med. Image Comput. Comput. Interv. 2012 Work. Nov. Biomarkers Alzheimer's Dis. Relat. Disord. 2012
11. Detre JA, Rao H, Wang DJJ, et al. Applications of arterial spin labeled MRI in the brain. J Magn Reson imaging. 2012; 35:1026–1037. [PubMed: 22246782]
12. Du AT, Jahng GH, Hayasaka S, et al. Hypoperfusion in frontotemporal dementia and Alzheimer disease by arterial spin labeling MRI. Neurology. 2006; 67:1215–1220. [PubMed: 17030755]
13. Alsop DC, Dai W, Grossman M, Detre JA. Arterial Spin Labeling Blood Flow MRI: Its Role in the Early Characterization of Alzheimer's Disease. J Alzheimer's Dis. 2010; 20:871–880. [PubMed: 20413865]
14. Hu WT, Wang Z, Lee VM-Y, et al. Distinct cerebral perfusion patterns in FTLD and AD. Neurology. 2010; 75:881–888. [PubMed: 20819999]
15. Kandel BM, Wang DJJ, Detre JA, et al. Decomposing cerebral blood flow MRI into functional and structural components: A non-local approach based on prediction. Neuroimage. 2015; 105:156–170. [PubMed: 25449745]
16. Nestor PJ, Graham NL, Fryer TD, et al. Progressive non-fluent aphasia is associated with hypometabolism centred on the left anterior insula. Brain. 2003; 126:2406–2418. [PubMed: 12902311]
17. Baron JC, Bousser MG, Comar D, Castaigne P. "Crossed cerebellar diaschisis" in human supratentorial brain infarction. Trans Am Neurol Assoc. 1981; 105:459–461. [PubMed: 19645126]
18. Zhou J, Gennatas ED, Kramer JH, et al. Predicting Regional Neurodegeneration from the Healthy Brain Functional Connectome. Neuron. 2012; 73:1216–1227. [PubMed: 22445348]
19. Jucker M, Walker LC. Self-propagation of pathogenic protein aggregates in neurodegenerative diseases. Nature. 2013; 501:45–51. [PubMed: 24005412]
20. Crossley NA, Mechelli A, Scott J, et al. The hubs of the human connectome are generally implicated in the anatomy of brain disorders. Brain. 2014; 137:2382–2395. [PubMed: 25057133]
21. Buckner RL, Sepulcre J, Talukdar T, et al. Cortical hubs revealed by intrinsic functional connectivity: mapping, assessment of stability, and relation to Alzheimer's disease. J Neurosci. 2009; 29:1860–1873. [PubMed: 19211893]
22. Wu W-C, Fernández-Seara M, Detre JA, et al. A theoretical and experimental investigation of the tagging efficiency of pseudocontinuous arterial spin labeling. Magn Reson Med. 2007; 58:1020–1027. [PubMed: 17969096]
23. Gorno-Tempini ML, Hillis AE, Weintraub S, et al. Classification of primary progressive aphasia and its variants. Neurology. 2011; 76:1006–1014. [PubMed: 21325651]
24. Irwin DJ, McMillan CT, Toledo JB, et al. Comparison of cerebrospinal fluid levels of tau and Aβ 1–42 in Alzheimer disease and frontotemporal degeneration using 2 analytical platforms. Arch Neurol. 2012; 69:1018–1025. [PubMed: 22490326]
25. Tustison NJ, Cook PA, Klein A, et al. Large-scale evaluation of ANTs and FreeSurfer cortical thickness measurements. Neuroimage. 2014; 99:166–179. [PubMed: 24879923]
26. Klein A, Ghosh SS, Avants B, et al. Evaluation of volume-based and surface-based brain image registration methods. Neuroimage. 2010; 51:214–220. [PubMed: 20123029]
27. Avants BB, Epstein CL, Grossman M, Gee JC. Symmetric Diffeomorphic Image Registration with Cross- Correlation: Evaluating Automated Labeling of Elderly and Neurodegenerative Brain. Med Image Anal. 2008; 12:26–41. [PubMed: 17659998]

28. Avants BB, Tustison N, Song G, Cook P. A Reproducible Evaluation of ANTs Similarity Metric Performance in Brain Image Registration. Neuroimage. 2011; 54:2033–2044. [PubMed: 20851191]
29. Das SRSSR, Avants BB, Grossman M, Gee JCJ. Registration based cortical thickness measurement. Neuroimage. 2009; 45:867–879. [PubMed: 19150502]
30. Satterthwaite TD, Shinohara RT, Wolf DH, et al. Impact of puberty on the evolution of cerebral perfusion during adolescence. Proc Natl Acad Sci U S A. 2014; 111:8643–8648. [PubMed: 24912164]
31. Avants BB, Lakshmikanth SK, Duda JT, et al. Robust cerebral blood flow reconstruction from perfusion imaging with an open-source, multi-platform toolkit. Int Soc Magn Reson Med Sci Work Perfus MRI Stand Beyond CBF Everyday Clin Appl. 2012; 21
32. Johnson NA, Jahng G-H, Weiner MW, et al. Pattern of Cerebral Hypoperfusion in Alzheimer Disease and Mild Cognitive Impairment Measured with Arterial Spin-labeling MR Imaging: Initial Experience. Radiology. 2005:851–859. [PubMed: 15734937]
33. Winkler AM, Ridgway GR, Webster MA, et al. Permutation inference for the general linear model. Neuroimage. 2014; 92:381–397. [PubMed: 24530839]
34. Newhart M, Ken L, Kleinman JT, et al. Neural networks essential for naming and word comprehension. Cogn Behav Neurol. 2007; 20:25–30. [PubMed: 17356341]
35. Friederici A, Rueschemeyer S. The role of left inferior frontal and superior temporal cortex in sentence comprehension: localizing syntactic and semantic processes. Cereb Cortex. 2003; 13:170–177. [PubMed: 12507948]
36. Bolling DZ, Pitskel NB, Deen B, et al. Dissociable Brain Mechanisms for Processing Social Exclusion and Rule Violation. Neuroimage. 2011; 54:2462–2471. [PubMed: 20974272]
37. Furl N, Averbeck BB. Parietal Cortex and Insula Relate to Evidence Seeking Relevant to Reward-Related Decisions. J Neurosci. 2011; 31:17572–17582. [PubMed: 22131418]
38. Kim E-J, Sidhu M, Gaus SE, et al. Selective frontoinsular von Economo neuron and fork cell loss in early behavioral variant frontotemporal dementia. Cereb Cortex. 2012; 22:251–259. [PubMed: 21653702]
39. Rosen HJ, Gorno-Tempini ML, Goldman WP, et al. Patterns of brain atrophy in frontotemporal dementia and semantic dementia. Neurology. 2002; 58:198–208. [PubMed: 11805245]
40. Dukart J, Mueller K, Horstmann A, et al. Differential effects of global and cerebellar normalization on detection and differentiation of dementia in FDG-PET studies. Neuroimage. 2010; 49:1490–1495. [PubMed: 19770055]
41. Edwards-Lee T, Miller BL, Benson DF, et al. The temporal variant of frontotemporal dementia. Brain. 1997; 120:1027–1040. [PubMed: 9217686]
42. Andoh J, Martinot J-L. Interhemispheric compensation: a hypothesis of TMS-induced effects on language-related areas. Eur psychiatry. 2008; 23:281–288. [PubMed: 18455371]
43. Halpern CH, Glosser G, Clark R, et al. Dissociation of numbers and objects in corticobasal degeneration and semantic dementia. Neurology. 2004; 62:1163–1169. [PubMed: 15079017]

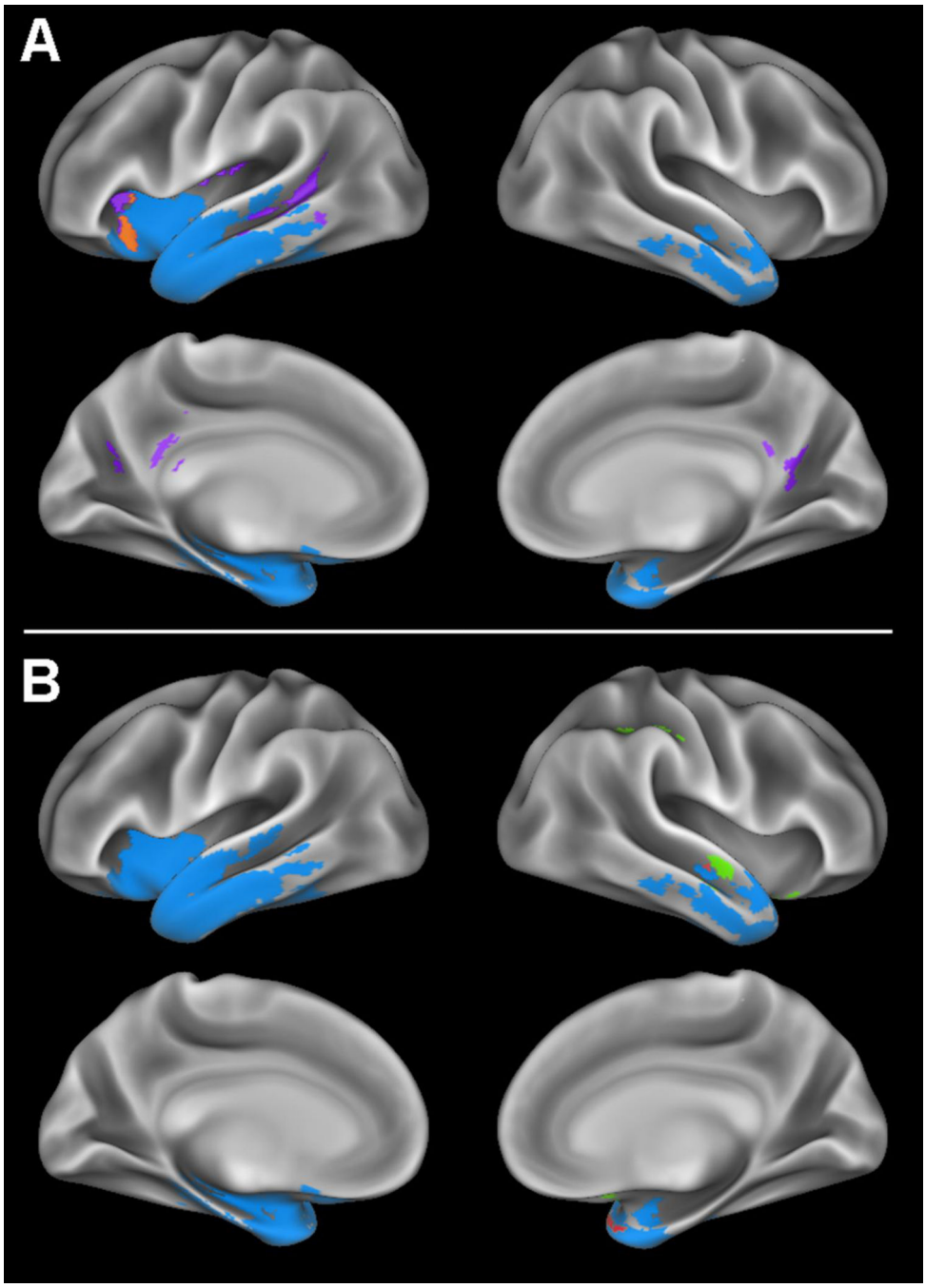

Figure 1. Whole-brain cortical thickness and perfusion comparisons

A) Regions where patients with semantic variant primary progressive aphasia (svPPA) display gray matter thinning relative to controls are shown in blue, regions of partial volume corrected (PVC) hypoperfusion without gray matter thinning in svPPA are shown in purple, and a region displaying both PVC hypoperfusion and gray matter thinning relative to controls is shown in orange. B) Regions where patients with svPPA display gray matter thinning relative to controls are shown in blue, PVC hyperperfusion without gray matter

thinning in svPPA is shown in green, and regions where patients display both PVC hyperperfusion and gray matter thinning relative to controls are shown in red.

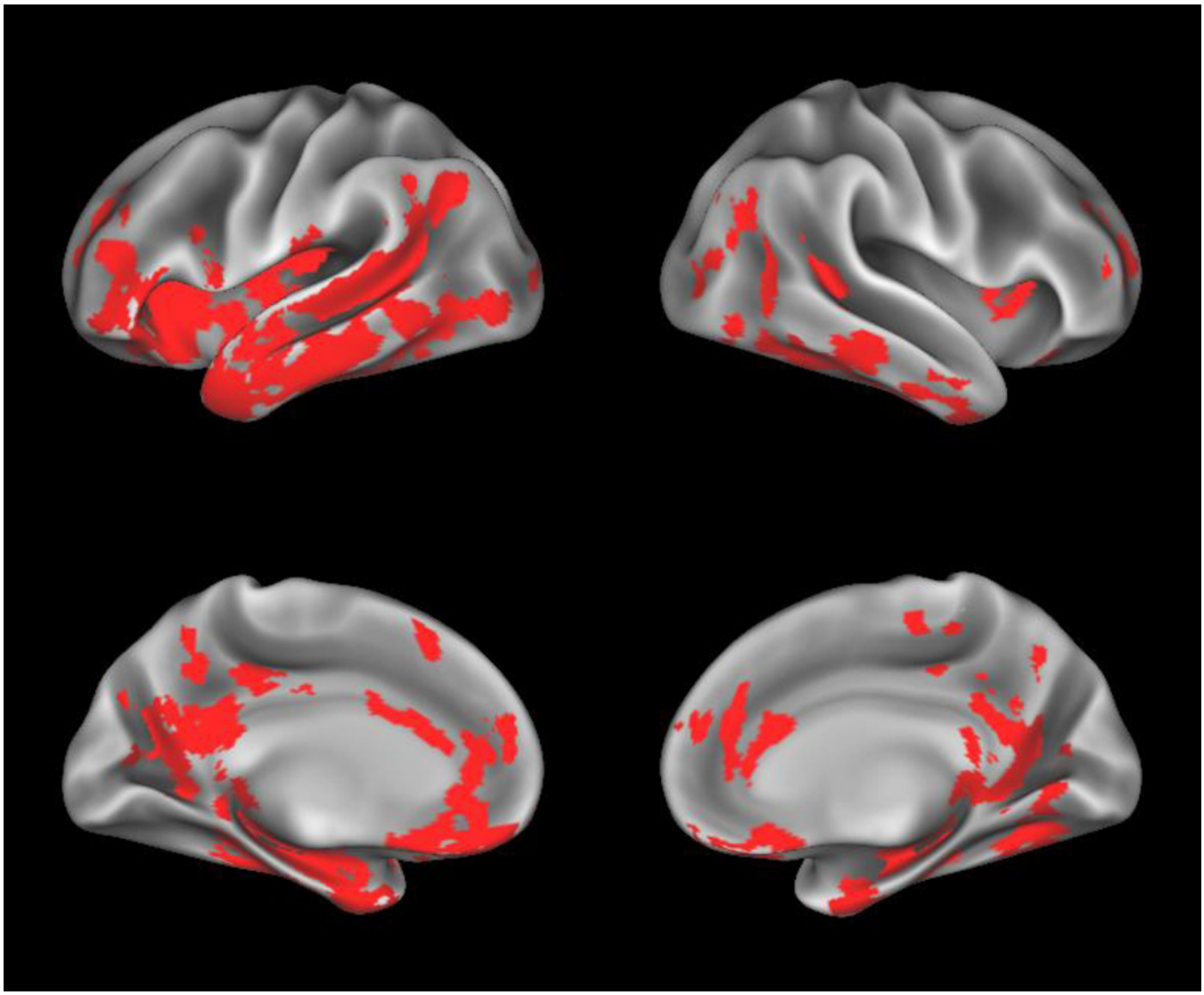

Figure 2. Whole-brain uncorrected perfusion comparisons

Regions where patients with semantic variant primary progressive aphasia (svPPA) display hypoperfusion relative to controls are shown in red.

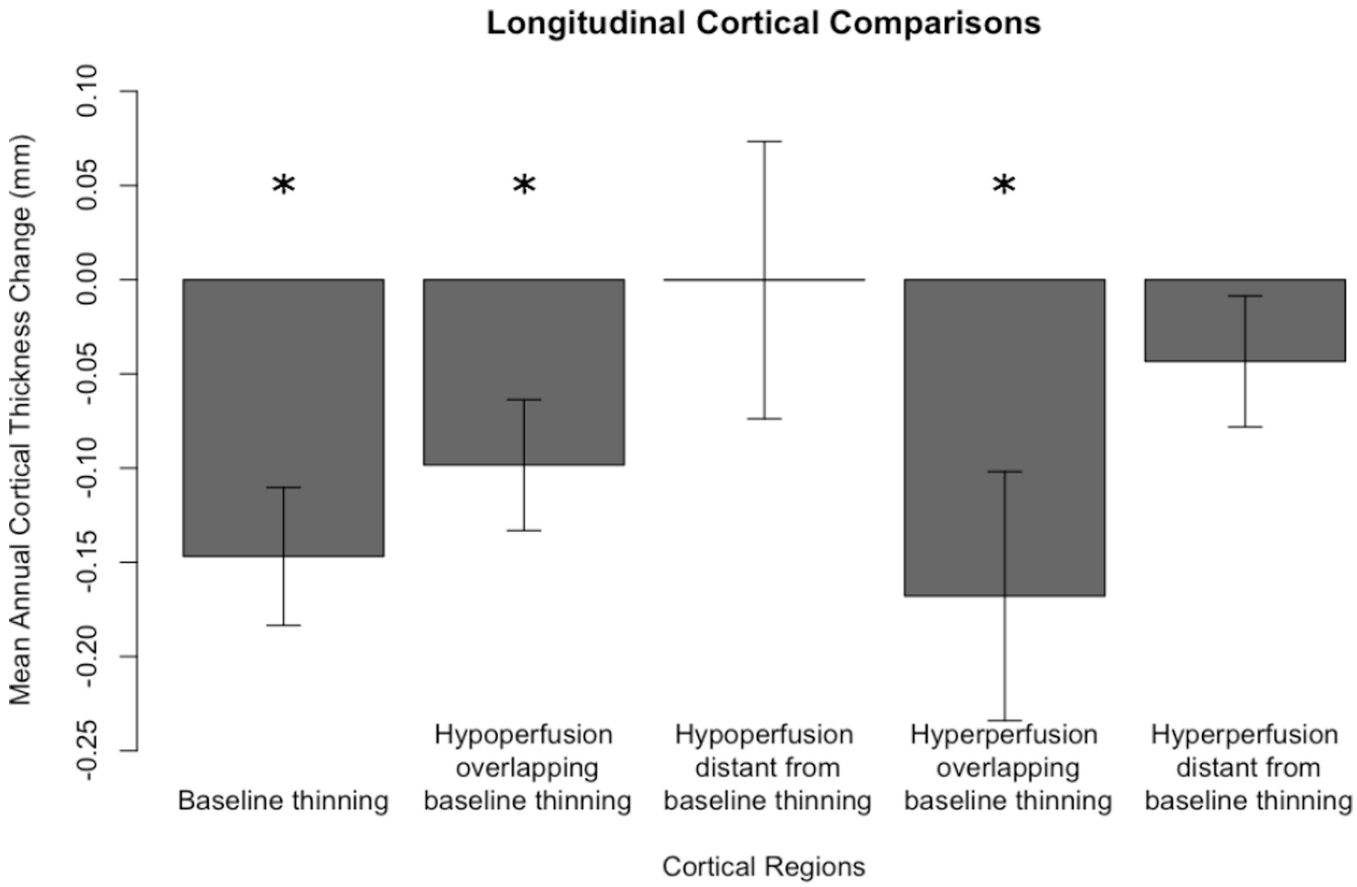

Figure 3. Longitudinal cortical thickness change

We calculated the mean (S.E.) annual cortical thickness change using baseline and follow-up cortical thickness MRI measurements in semantic variant primary progressive aphasia. The mean annual cortical thickness is measured within regions where patients displayed cortical baseline thinning, hypoperfusion partially overlapping thinning, hypoperfusion distant from thinning, hyperperfusion partially overlapping thinning, and hyperperfusion distant from thinning. Patients showed significant progressive thinning in regions of baseline thinning, regions of hypoperfusion near thinning, and hyperperfusion near regions of thinning ($p<0.05$ using paired-sampled t-tests, represented by *). Patients did not show progressive thinning in regions distant from thinning at baseline.

Table 1

Mean of semantic variant primary progressive aphasia (svPPA) patient and control participant demographic and clinical information.

Group	Control	svPPA
N (female)	19 (12)	13 (7)
Age (SE, Range)	65.2 (1.71, 53–78)	61.8 (2.06, 49–71)
Education (SE, Range)	15.6 (0.60, 12–20)	16.5 (0.75, 12–22)
Duration from symptom onset (SE, Range)	--	3.69 (0.12, 1–9)
MMSE (SE, Range) *	29.6 (0.16, 28–30)	22.7 (1.72, 14–30)
BNT Mean Z-score (N<−1.96, Range)	--	−14.7 (13, −16.1– −9.07)
Animals Mean Z-score (N<−1.96, Range)	--	−2.25 (11, −3.23– −0.80)
Digit Span Forward Z-score (N<−1.96, Range)	--	−0.54 (1, −3.14–0.83)
Digit Span Reverse Z-score (N<−1.96, Range)	--	−1.22 (2, −3.73–0.35)

Significant differences between controls and patients with svPPA indicated by * ($p=0.002$ using independent samples t-test). Patient z-scores for cognitive measures relative to healthy control data (z-score < −1.96 equivalent to $p<0.05$).

Abbreviations: N=number; SE=standard error; svPPA=semantic variant primary progressive aphasia; MMSE=mini-mental state examination; BNT=Boston naming test; N<−1.96=number of patients scoring significantly worse than controls ($p<0.05$)

J Neurol. Author manuscript; available in PMC 2017 October 01.

Table 2

Anatomic locations of gray matter hypoperfusion corrected for partial volume effects, hyperperfusion corrected for partial volume effects, and cortical thinning in patients with semantic variant primary progressive aphasia relative to controls. Also shown are anatomic locations where patient cortical thinning and hypoperfusion corrected for partial volume effects overlap and regions where patient cortical thinning and hyperperfusion corrected for partial volume effects overlap.

Anatomic Locus (Brodmann Area)	MNI Coordinates			Peak T-statistic	Cluster Volume (mm^3)
	x	y	z		
PATIENT HYPOPERFUSION (PEAK VOXEL)					
L middle temporal (21)	−53	−30	−5	5.41	2096
L anterior insula	−28	23	−6	3.77	720
L posterior insula	−42	−22	22	3.98	534
**L precuneus (7)	−13	−60	28	3.80	562
**R posterior cingulate (23)	2	−48	22	4.40	2051
PATIENT HYPERPERFUSION (PEAK VOXEL)					
R temporopolar (38)	31	16	−28	4.66	1479
*R orbitofrontal (11)	14	18	−14	--	--
R middle temporal (21)	59	−8	−13	4.98	1051
**R inferior parietal (40)	41	−41	44	4.34	856
PATIENT GRAY MATTER THINNING (PEAK VOXEL)					
L inferior temporal (20)	−26	−5	−43	21.9	65392
R temporopolar (38)	27	19	−39	9.36	20954
R inferior temporal (20)	54	−35	−16	6.00	879
PATIENT GRAY MATTER THINNING AND HYPOPERFUSION OVERLAP (CENTER OF CLUSTER)					
L superior temporal (22)	−61	−38	2	--	18
L anterior insula	−28	22	−8	--	365
L anterior insula	−29	17	7	--	13
PATIENT GRAY MATTER THINNING AND HYPERPERFUSION OVERLAP (CENTER OF CLUSTER)					
R temporopolar (38)	32	17	−29	--	655
R temporopolar (38)	27	10	−25	--	1
R middle temporal (21)	55	−12	−13	--	236

* Represents subpeak.

** Represents cluster "distant" from cortical thinning